Polymer-Inorganic Coatings Containing Nanosized Sorbents Selective to Radionuclides. 1. Latex/Cobalt Hexacyanoferrate(II) Composites for Cesium Fixation

Svetlana Bratskaya,*,[†] Anna Musyanovych,[‡] Veniamin Zheleznov,[†] Alla Synytska,[§] Dmitry Marinin,[†] Frank Simon,[§] and Valentin Avramenko[†]

[†]Institute of Chemistry Far Eastern Branch of the Russian Academy of Sciences, Prosp.100-letiya Vladivostoka 159, 690022 Vladivostok, Russia

[‡]Max Planck Institute for Polymer Research, Ackermannweg 10, 55128 Mainz, Germany

[§]Leibniz-Institut für Polymerforschung Dresden e.V., Hohe Str. 6, 01069 Dresden, Germany

S *Supporting Information*

ABSTRACT: Here we present a new approach to improve fixation of radionuclides on contaminated surfaces and eliminate their migration after nuclear accidents. The approach consists in fabrication of latex composite coatings, which combine properties of polymeric dust-suppressors preventing radionuclides migration with aerosols and selective inorganic sorbents blocking radionuclides leaching under contact with ground waters and atmospheric precipitates. Latex/cobalt hexacyanoferrate(II) (CoHCF) composites selective to cesium radionuclides were synthesized via "in situ" growth of CoHCF crystal on the surface of carboxylic or amino latexes using surface functional groups as ion-exchange centers for binding precursor ions Co^{2+} and $[Fe(CN)_6]^{4-}$. Casting such composite dispersions with variable content of CoHCF on ^{137}Cs-contaminated sand has yielded protective coatings, which reduced cesium leaching to 0.4% compared to 70% leaching through original latex coatings. ^{137}Cs migration from the sand surface was efficiently minimized when the volume fraction of CoHCF in the composite film was as low as 0.46−1.7%.

KEYWORDS: ^{137}Cs, ferrocyanide, nanoparticles, radionuclide migration, soil, dust suppressor
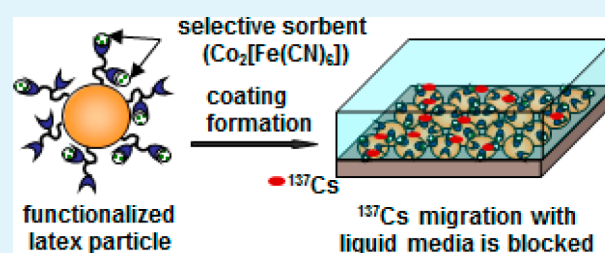
1. INTRODUCTION

Presently, latex organic−inorganic composites keep gaining academic and industrial interest due to a wide range of possible applications and a beneficial combination of polymer properties with inorganic materials functionality.[1−4] Inorganic nanoparticles can be incorporated into latexes during polymerization process,[3] attached to the latex surface via electrostatic, hydrogen, or covalent bonding,[2] or "in situ" deposited on the latex surface.[4] Such latex-inorganic composites have been already used for fabrication of coatings with high refractive index,[3] improved hardness, water and stain resistance,[2,5] self-sterilizing,[6] and many others useful properties. To the best of our knowledge, latex coatings containing sorbents selective to radionuclides have not been previously reported, although hybrid polymer-inorganic thin films for selective adsorption and subsequent determination of radionuclides are known to the researchers.[7] However, the interest in such materials is far beyond the narrow field of analytical preconcentration of radionuclides.

We have recently shown[8] that nanoparticles of selective inorganic sorbents can be immobilized to latex particles and applied as "liquid" or colloidal stable sorbents for cesium recovery from solutions and contaminated solid materials.

Extending this approach to film-forming latexes can be used for fabrication of a new type of dust suppressing coatings, which would combine properties of protective polymer film and selective sorbent to increase efficiency of radionuclides fixation after nuclear accidents. Application of polymeric dust-suppressors became a general practice allowing radionuclides entrapment within thin polymer films on the surfaces contaminated after accidents on nuclear power plants (NPP), radiochemical plants, and weapon production facilities.[9] Such measures help to securely eliminate migration of radionuclides with aerosols, but do not limit their mobility in solid phase under high humidity conditions due to solubility of the water-based polymer products[10] or permeability of the latex coatings for small ions, including radionuclides.[11] This limits effective long-term open-air application of dust-suppressor, since under continuous exposure to atmospheric precipitations radionuclides can migrate from soil surface deep into the soil profiles.

Table 1. Characteristics of the Latexes

latex	composition	diameter nm	ζ potential mV	content of ionic groups per NP	per nm^2	mmol/g of latex	theoretical capacity for CoHCF mmol/g
SL	polystyrene	162 ± 12	−8 ± 3	0	0		
ASL-1	poly(styrene/AA)	166 ± 15	−23 ± 5	24 820	0.41	0.0236	0.0059
ASL-5		157 ± 25	−35 ± 8	81 159	1.59	0.0974	0.0243
ASL-6		164 ± 9	−37 ± 6	225 762	3.37	0.184	0.0460
ASL-10		244 ± 47	−41 ± 9	409 998	3.50	1.44	0.3600
BMMDS-0.3	poly(MMA/BA/DMVS/MAA)	142 ± 15	−30 ± 7	74 215	1.17	0.0787	0.0190
BMMDS-0.06		119 ± 13	−17 ± 5	18 652	0.31	0.0336	0.0084
BMADS-0.3	poly(MMA/BA/DMVS/AEMA)	98 ± 15	+27 ± 5	41 267^a	0.98^a	0.133^a	0.1330
BMADS-0.06		105 ± 12	+3 ± 1	13 455^a	0.37^a	0.0018^a	0.0018

^{a}related to content of amino groups, all other values are related to carboxylic groups.

Long-lived radionuclides released after the nuclear accidents not only pose direct serious health threats for inhabitants, but also exclude large territories from agricultural use for many years. Immediately after the contact with the soil surface, ^{134}Cs and ^{137}Cs radionuclides, which are of great concern due to their strong photon energies and long half-lives, are mainly localized at a depth of up to 5 cm.[12,13] However, the rate of their downward migration in the soil is on average 1 cm/year[14] and largely depends on the soil structure and composition. For example, the migration depth of cesium radionuclides in soils of Scotland exceeded 17 cm 23 years after the Chernobyl accident.[15] Usually, the remediation activity starts several months after the accidents, and the amount of soil that must be removed afterward depends on how efficient were the first measures on prevention of radionuclides migration to deeper ground layers.[16]

The aim of the present work was to develop a new approach to improve fixation of radionuclides on contaminated surface, including soils and grounds, and prevent their migration under high humidity conditions. The approach is based on application of recently reported[8] type of the latex composites containing inorganic selective sorbents, for example, cobalt hexacyanoferrate(II) selective to cesium ions,[17] to form on contaminated surfaces composite dust-suppressing coatings minimizing cesium leaching to the environment.

2. EXPERIMENTAL SECTION

2.1. Chemicals and Reagents. Styrene (St) purchased from Merck and butyl acrylate (BA), methyl methacrylate (MMA), methacrylic acid (MAA), and acrylic acid (AA) purchased from Aldrich were distilled under reduced pressure and stored at −20 °C before use. Other reagents and solvents were used as received: diethoxy(methyl)vinyl silane (DMVS, Aldrich), aminoethyl methacrylate hydrochloride (AEMA, Aldrich), the hydrophobic initiator 2,2′-azobis(2-methylbutyronitrile) (V59, Wako-Chemicals), the hydrophobe hexadecane (Aldrich), a nonionic surfactant Lutensol AT50 - poly(ethylene oxide)-hexadecyl ether with an ethylene oxide block length of about 50 units (BASF).

2.2. Latex Synthesis. All latexes used in the present work were synthesized by free radical copolymerization in the direct (oil in water) miniemulsion system.[18] Briefly, 0.250 g of hexadecane, 100 mg of V59, and different amounts of monomers (except AEMA) were mixed together and added to the aqueous phase consisting of 24 g of demineralized water and 0.400 g of Lutensol AT50. For the synthesis of amino-functionalized latexes, AEMA was dissolved in the aqueous phase and then mixed with the oil (dispersed) phase. The amount of monomers used for the latex preparations is given in Supporting Information, Table S1.

Both phases were stirred together for 1 h at 1000 rpm for pre-emulsification, and the miniemulsion was prepared by ultrasonicating

the mixture for 120 s at 90% intensity (Branson sonifier W450 Digital, 1/2″ tip) at 0 °C to prevent polymerization. Afterward, the mixture was transferred into a round-bottom flask, which was then closed and placed into the oil bath at 72 °C. The reaction proceeded overnight under magnetic stirring at 600 rpm. After synthesis the latexes were purified from the surfactant excess by multiple centrifugation/redispersion in demineralized water and characterized in terms of particle size, zeta potential, and functional groups density. The characteristics of the latexes are summarized in Table 1.

2.3. Composite and Coatings Preparation. To obtain composites, cobalt hexacyanoferrate (II) (CoHCF) was immobilized to carboxylic latexes by successive addition of aliquots of 0.01 M CoCl$_2$ and 0.005 M K$_4$[Fe(CN)$_6$] solutions to a latex dispersion with solid content of 0.5%, 2%, 5%, or 10% at pH = 5.2−5.4. When composites were prepared from amino latexes, reagents were added in the reversed sequence. Theoretical chemical composition of CoHCF in latex/CoHCF composite was Co$_2$[Fe(CN)$_6$]; the actual chemical composition was determined as a difference between content of K, Na, Fe, and Co in stable dispersion and in supernatant after precipitation of latex/CoHCF composite by centrifugation at 14 000 rpm, 60 min. Metal contents were determined by atomic absorption spectroscopy using Solaar 6 M spectrometer (Thermo, USA). The CoHCF for all composites is given in Supporting Information, Table S2. For simplicity, taking into account small differences in composition of cobalt hexacyanoferrates, in all cases we will refer to a general notation, CoHCF. CoHCF content was varied from 2×10^{-5} to 0.06 mmol per 1 g of dry latex, and in all cases was calculated on the basis of Fe content. All composites were labeled as "latex name"/CoHCF, for example, ASL-1/CoHFC, which indicates composite prepared by immobilization of CoHCF in ASL-1 latex.

Coatings were fabricated by casting 0.2 mL of dispersions with the latex solid content of 2%, 5%, or 10% on the silicon wafer (for SEM measurements) or on double-sided adhesive tape covered with ^{137}Cs-spiked quartz sand (for ^{137}Cs leaching tests). All samples had geometrical surface area 5.29 cm^2. The volume fraction of CoHCF in composite coatings was calculated according to the following formula:

$$\phi = (C_{CoHCF} \cdot V_l \cdot C_l \cdot Mr_{CoHCF} / h_{film} \cdot S_{film} \cdot \rho_{CoHCF}) \cdot 100\%$$

where C_{CoHCF} is CoHCF content in composite, mol per 1g of the latex; Mr_{CoHCF} is molecular weight of CoHCF, C_l is latex solid content in composite dispersion, g/L; V_l is casted volume of the latex/CoHCF composite dispersion, L; h_{film} is coating thickness, cm; S_{film} is film area, cm^2; ρ_{CoHCF} is CoHCF density (1.89 g/cm^3).

2.4. Characterization of the Latex Particles and the Latex/CoHCF Composites. The size and electrokinetic potential of the latex particles and the latex/CoHCF composites were determined in a 0.0001 M KCl solution at pH 6.4 and pH 5.4, respectively, by the photon correlation spectroscopy and laser Doppler electrophoresis methods on a Malvern ZetaSizer Nano ZS analyzer (typical correlation functions and size distributions for original latexes and composites are presented in Supporting Information, Figures S1 and S2). The content of −COOH and −NH$_2$ groups were determined by colloid titration using a particle charge detector PCD 02 (Mütek GmbH, Germany) in

combination with a 702 SM Titrino (Metrohm AG, Switzerland) automatic titrator.[18]

The stability of latex/CoHCF composites was studied in 0.5% latex dispersions by quantifying the iron in aliquots of dispersion sampled from the surface of the liquid in a cylinder at fixed time intervals (the height of the liquid column was 5 cm). The stability of CoHCF dispersion prepared in distilled water was investigated for comparison. The iron content was determined by atomic absorption spectroscopy on a Solaar 6 M spectrometer (Thermo, USA).

2.5. Characterization of the Latex and the Latex/CoHCF Composite Coatings. *Scanning Electron Microscopy (SEM).* All SEM images illustrating morphology and topography of original latex and latex/CoHCF composite coatings were acquired on a NEON 40 EsB Crossbeam scanning electron microscope from Carl Zeiss NTS GmbH, operating at 3 kV in the secondary electron (SE) mode. To enhance the electron density contrast, samples were coated with platinum (3.5 nm) using a Leica EM SCD500 sputter coater. The coating thickness was determined from cross-section SEM images after drying for 24 h at room temperature.

Transmission Electron Microscopy (TEM). A drop of the latex/CoHCF composite dispersion containing 0.035 mmol of CoHCF per 1 g of latex was placed on a TEM grid and dried under ambient conditions. Copper grids covered with a holey carbon film (200 mesh, Quantifoil R1.2/1.3) were used for the analysis (Quantifoil GmbH, Germany). TEM images were taken with a Libra 200 TEM (Carl Zeiss Microscopy, Germany), equipped with a field emission gun (FEG) running at an acceleration voltage of 200 kV. The in-column energy filter with an energy window of 20 eV was used. The images were recorded on a 4k camera (TVIPS GmbH, Germany) in 2 × 2 binning mode and adjusted in contrast and brightness using iTEM software (Olympus, Japan).

X-ray powder diffraction analysis was carried out on a Dron-3 multipurpose diffractometer on the coating fabricated by spreading 2 mL of latex/CoHCF composite dispersion (latex content 2%, CoHCF content 0.035 mmol per 1 g of dry latex) on quartz crystal plate. The coating thickness was ~50 μm.

The wettability of latex and latex/CoHCF composite coatings was investigated using contact angle measurements. Advancing and receding water contact angles were measured by the sessile drop method using a conventional drop shape analysis technique (Krüss DSA 10, Hamburg, Germany). Deionized reagent grade water was used for contact angle measurements. All contact angle measurements were carried out at 24 ± 0.5 °C and relative humidity of 40 ± 3%, which were kept constant.

2.6. ^{137}Cs Leaching Test. Quartz sand (fraction 0.100−0.315 mm) preliminarily cleaned with a 0.1 M HCl solution and thoroughly washed was used to imitate the contaminated solid surface. To spike sand with cesium radionuclides, it was wetted with a solution containing ^{137}Cs, left until dry, and averaged over the volume. The resulting γ-activity of the sand sample was ~2000 Bq/g.

To obtain reliably fixed monolayers of sand particles, 60−70 mg of the ^{137}Cs-spiked sand was homogeneously distributed over 5.29 cm^2 piece of a double-sided adhesive tape attached into a Petri dish. The initial γ-activity of each sample was measured. The coatings on sand surfaces were formed as described in Section 2.3 and dried for 24 h prior to ^{137}Cs leaching experiments. Then 5 mL of distilled water or NaCl solution was introduced into the Petri dish and left without shaking for 24 h (or for the fixed time from 10 min to 10 d when studying the kinetics of the process). The ^{137}Cs distribution between the leaching solution and the solid phase was monitored by measuring the residual γ-activity of the quartz sand. In addition, the γ-activity of the solution was measured to ensure better γ-activity control.

The γ-activity of the ^{137}Cs γ radiation was determined by the direct spectrometric method from the line $E\gamma = 662$ keV with the use of a Gamma 1C universal spectrometer (Aspekt Research and Production Center, Russia). The γ activity of the samples was measured taking into account the "dead time" of the equipment. The counting rates were not higher than 10 000 counts/s. The specific activity of ^{137}Cs γ radiation in a solution was measured in 5 mL volume. The activity of solid samples after leaching was measured directly in the Petri dish for

point geometry. The conversion factor (k) from the point radiation source to a bulk sample (5 mL) was determined from the ratio of the ^{137}Cs counting rate in a drop of a radioactive solution to the counting rate after dilution and was equal to 1.41.

The amount of ^{137}Cs leached from the sand surface was estimated as

$$L = (A_{leached}/A_0) \cdot 100\%$$

where A_0 is initial total γ activity of the solid sample, $A_{leached}$ is total γ activity of the solid sample after leaching. When $A_{leached}$ was determined by analyzing γ activity of the solution ($A_{solution}$), it was calculated as $A_{leached} = k \cdot A_{solution}$. The difference between L values calculated using γ activity of solid phase and liquid phase was in the range of 1−3%.

3. RESULTS AND DISCUSSION

3.1. General Concept of Composite Coatings for Radionuclides Fixation on Contaminated Surface. The general concept of the suggested approach is illustrated in Figure 1 and consists in fabrication of latex composite coatings
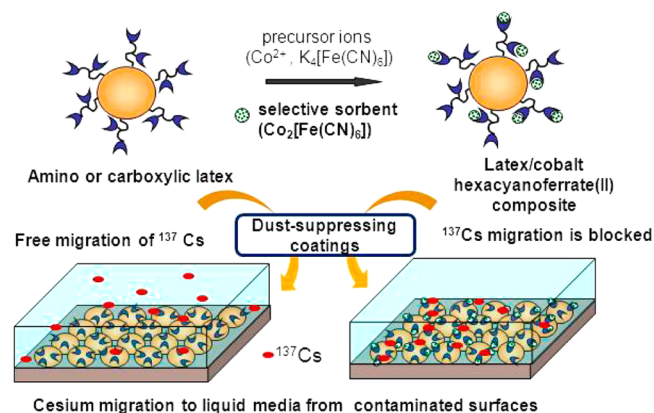

Figure 1. General concept of latex/cobalt hexacyanoferrate(II) (CoHCF) composites application for fabrication of coatings preventing cesium leaching and migration from contaminated surface.

containing nanosized sorbents with high selectivity to radionuclides. We suggest that such coatings, combining dust-suppressing properties of the latexes and sorption properties of the inorganic materials, can be obtained by spraying or casting dispersions of latex/sorbents composites on the contaminated surface. The colloidal stable latex/sorbent composites can be obtained either by electrostatic attachment of "ex situ" synthesized sorbents nanoparticles to the latex surface or by "in situ" growth of sorbent nanocrystals on the latex surface using surface functional groups as ion-exchange centers for binding precursor ions. One example of such composites containing hexacyanoferrates(II) of several transition metals we have demonstrated recently.[8] The similar approach based on anchoring of the metal precursor on the reactive organic groups was used for fabrication of porous RuO$_2$@SiO$_2$ hybrids.[19]

The main idea of the suggested approach here is based on the assumption that the presence of the selective sorbent nanoparticles in composite coatings can reduce permeability of the latex film for target radionuclides and significantly decrease radionuclides migration rate under the contact with atmospheric precipitates or ground waters.

Here we will focus on application of latex composites containing CoHCF, which is very selective to cesium ions,[16] for fabrication of coatings assuring efficient fixation of cesium on

contaminated surfaces and preventing its leaching and migration under contact with liquid media. To implement the suggested concept the following main questions will be addressed: (i) which types of functional groups can be used for fixation of CoHCF on the latex surface; (ii) how does the content of latex surface groups effect colloidal stability of the latex/CoHCF composite, (iii) what content of CoHCF in composite is required to provide efficient fixation of cesium after casting latex/CoHCF composite dispersion on contaminated surface?

3.2. Fabrication and Properties of Latex/CoHCF Composites.

To elucidate requirements to latex surface characteristics, which are important for formation of stable composites with CoHCF, a series of carboxylic and amino latexes varying in content of surface functional groups has been synthesized (Table 1).

Since colloids of CoHCF have negative electrokinetic potential,[8] they cannot be bound to carboxylic latexes via electrostatic interactions but can be formed on the latex surface via the "in situ" growth mechanism. At the first stage of this process, Co^{2+} ions bind to the latex carboxylic groups in the pH range of 5.2−5.4, where carboxylic groups are nearly completely ionized (Supporting Information, Figure S3), and formation of cobalt hydroxides is not yet started. At the second stage, addition of $[Fe(CN)_6]^{4-}$ initiates the formation of insoluble complex of CoHCF and crystal growth from the latex surface, if the content of carboxylic groups is sufficiently high to ensure nanocrystal attachment and stabilization.

As a criterion of the latex/CoHCF composite stability, we used the iron content in the top layer of the dispersion, which remained constant, when no phase separation between latex and CoHCF colloids occurred, or decreased, when unstabilized CoHCF precipitated. Figure 2 shows that CoHCF rapidly
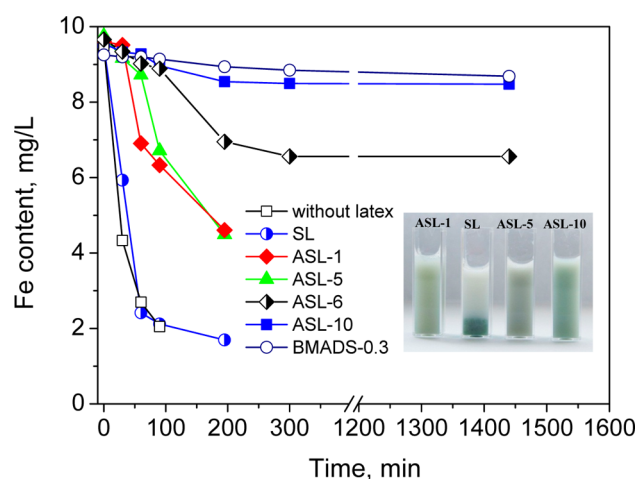

Figure 2. Kinetics of cobalt hexacyanoferrate(II) settling in latex/CoHCF composite dispersions fabricated from latexes with different content of surface functional groups (pH = 5.4, latex solid content 0.5%, CoHCF content 0.035 mmol per 1 g of the latex). Photo of the latex/CoHCF composite dispersions 3 h after fabrication.

precipitates in water and in dispersion of SL/CoHCF composite formed with polystyrene latex (SL), which does not contain any ion-exchange sites on the surface. The stability of latex/CoHCF composites significantly increases when carboxylic latexes were used for CoHCF immobilization: the

higher the surface group content was, the better the composite stability was (Figure 2).

Assuming that two carboxylic groups interact with one Co^{2+} ion and cobalt ferrocyanide has the composition close to $Co_2[Fe(CN)_6]$, the theoretical capacity of carboxylic latex for $Co_2[Fe(CN)_6]$ is 4 times lower than the content of carboxylic groups (Table 1). However, the amount of CoHCF, which can be loaded without loss of composite stability, is noticeably lower than the theoretical latex capacity for CoHCF. For example, up to 0.025 mmol cobalt ferrocyanide can be stabilized in 1 g of latex with the theoretical capacity for CoHCF 0.046 mmol/g (ASL-6). The same tendency was observed for other carboxylic latexes (Supporting Information, Figure S4). This suggests that the distance between surface groups can also play a significant role in attachment of CoHCF to the latex surface. At low content of carboxylic groups and large distance between ion-exchange sites, two adjusting carboxylic groups cannot be involved in stoichiometric surface complexation reactions with one Co^{2+} ion, so the attachment of CoHCF nanocrystals to the latex surface is relatively weak. The most stable composites were obtained when the content of carboxylic groups was at least 5 times higher than theoretically required for CoHCF binding. The most stable composites were obtained for the latex ASL-10 with the carboxylic groups content 1.44 mmol/g.

Only moderate changes in electrokinteic potential of composites were detected with the increase of CoHCF content (Figure 3), since the decrease of carboxylic groups surface charge due to the Co^{2+} ions binding is compensated by subsequent formation of negatively charged CoHFC colloids. The size of composites significantly increases only for ASL-10 latex with the highest content of carboxylic groups. The invariable size of all other composites can be attributed either to formation of very small ferrocyanide nanocrystals on the latex surface, so that the composite sizes remain within the experimental error of dynamic light scattering (∼10%), or to coexistence of free latex particles and CoHCF colloids.

TEM images of composites confirm (Figure 4) that polystyrene latex (SL) and latex with low content of carboxylic groups (ASL-1) do not form composites with CoHCF. Primary particles of CoHCF in these dispersions have the size ∼20 nm and are not attached to the latex surface. Thus, composites SL/CoHCF and ASL-1/CoHCF can be considered only as mixtures of two types of particles. CoHCF particles in these dispersions form a continuous network (Figure 4A,B) that results in fast phase separation in composite and CoHCF precipitation, as observed in Figure 2. Structure of ASL-10/CoHCF composite is completely different (Figure 4C): one observes neither primary CoHCF particles nor free latex particles. The composite contains only irregularly shaped particles with the size slightly larger than that of the latex. High-resolution TEM images show that shape irregularity results from formation of CoHCF layer around the latex particles that proves formation of ASL-10/CoHCF composite. Such composites containing up to 0.07 mmol of CoHCF per 1 g of latex remain stable at least over 4 months.

CoHCF can be also stabilized in dispersions of amino latexes (BMADS-0.3, Figure 2). Since $[Fe(CN)_6]^{4-}$ ions efficiently interact with aminopolymers,[20] an anion-exchange reaction can be used to initiate subsequent in situ growth of CoHCF crystals upon Co^{2+} addition. In contrast to carboxylic latexes, negative charge of CoHCF colloids compensates positive charge of the latex surface and composite loses stability at a certain content of
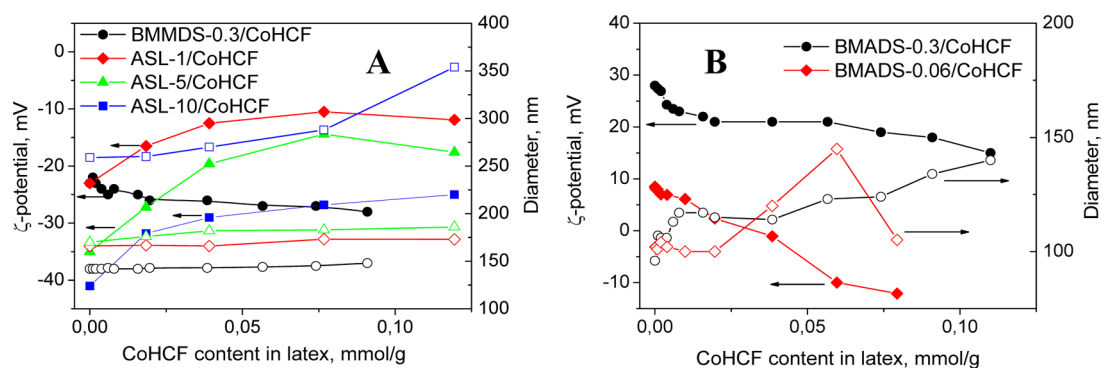
Figure 3. Electrokinetic potentials and particle sizes of carboxylic (A) and amino (B) latex/CoHFC composites (pH = 5.4, 0.001 M KCl). Closed symbols: ζ-potential, open symbols: diameter.
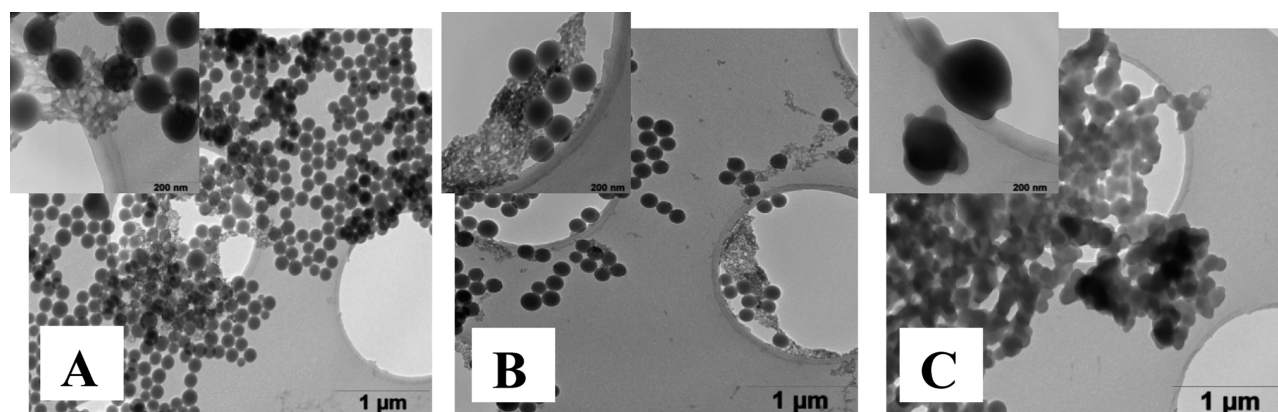

Figure 4. TEM images of latex/CoHFC composites containing 0.035 mmol $Co_2[Fe(CN)_6]$ per 1 g of the latex: SL (A), ASL-1 (B), ASL-10 (C).
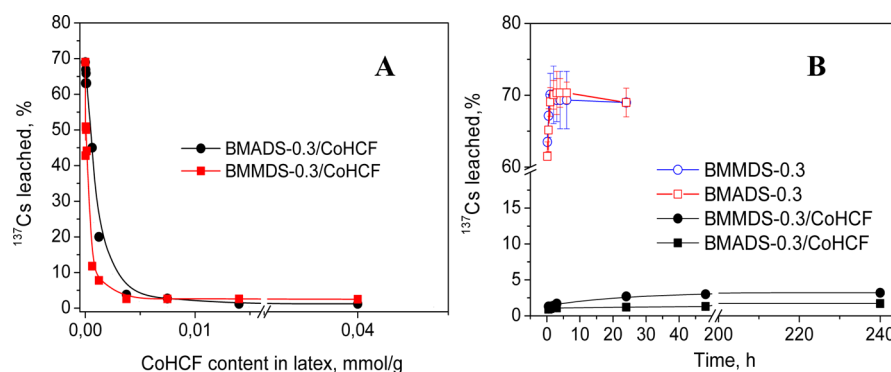

Figure 5. ^{137}Cs leaching with water from contaminated sand surface coated with latex/CoHCF composites varying in CoHCF content (A). Kinetics of ^{137}Cs leaching from contaminated sand surface coated with original latexes and latex/CoHCF composites containing 0.035 mmol CoHCF per 1 g of latex (B).

CoHCF. Because of the charge reversal, composites based on latex BMADS-0.06 with low content of amino groups are unstable at a CoHCF content of 0.025−0.06 mmol per 1 g of latex (Figure 3B, Supporting Information, Figure S5), while BMADS-0.3/CoHCF composite remained stable even when CoHCF content was increased to 0.11 mmol per 1 g of the latex.

3.3. Fabrication and Properties of Latex/CoHCF Composite Coatings. In contrast to polystyrene-based latexes, which are not film-forming, copolymers of acrylics and styrene with siloxanes and silanes are widely used in protective coatings due to their enhanced adhesion to the surface and water repellence.[21,22] In the present work, latex/CoHCF composites applicable for formation of dust-suppress-

ing coatings were fabricated using a series of copolymer latexes consisting of butyl acrylate, methyl methacrylate, diethoxy-(methyl)vinyl silane, and different concentrations of methacrylc acid or aminoethyl methacrylate units (Table 1). Here, we were aimed to find an optimum content of the selective sorbent in the latex/CoHCF composite to be used for fabrication of coatings preventing cesium migration with liquid media from ^{137}Cs-contaminated surface. This experiment simulates the behavior of dust suppressor films in open air under the effects of atmospheric precipitates and groundwater leaching.

To account for the effect of the latex type, composites were prepared using amino latex BMADS-0.3 and carboxylic latex BMMDS-0.3. Both BMMDS-0.3 and BMADS-0.3 original

Table 2. Effect of Latex/CoHCF Composite Coatings Characteristics on ^{137}Cs Leaching from Contaminated Sand

	latex	latex solid content, %	thickness, μm^a	CoHCF volume fraction,[b] %	leaching media	^{137}Cs leached, %[c]
1	BMMDS-0.3	2	2.95	0.63	water	5.0 ± 0.5
2		2		0.63	0.1 M NaCl	5.6 ± 0.5
3		2		0.63	0.5 M NaCl	10.4 ± 1
4		5	5.63	2.06	water	0.9 ± 0.2
5		10	27.03	1.72	water	0.5 ± 0.2
6	BMADS-0.3	2	4.03	0.46	water	1.2 ± 0.2
7		2		0.46	0.1 M NaCl	3.0 ± 0.3
8		2		0.46	0.5 M NaCl	4.8 ± 0.5
9		5	5.74	2.02	water	1.0 ± 0.2
10		10	29.53	1.57	water	0.4 ± 0.2

^{a}Film thickness was calculated from cross-section SEM images. ^{b}The CoHCF content in composites is fixed to 0.014 mmol per 1 g of latex. ^{c}Leached with water after 24 h.
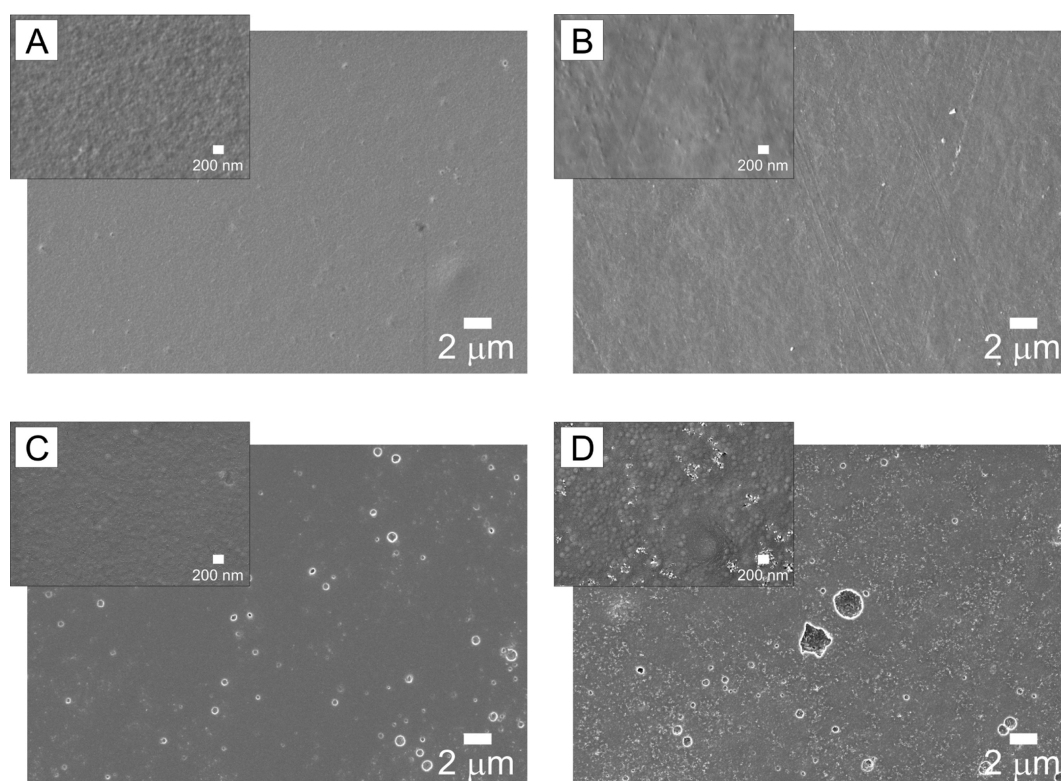

Figure 6. SEM images of coatings casted from 2% latex dispersions on silicon wafers: BMMDS-0.3 (A), BMADS-0.3 (B), BMMDS-0.3/CoHCF (C), BMADS-0.3/CoHCF (D). CoHCF content in all composites was 0.035 mmol per 1 g of latex.

latexes give hydrophilic coatings (advancing contact angles (θadv) = 59° and 54°, respectively), which are highly permeable for ^{137}Cs radionuclides. Investigations of the ^{137}Cs-leaching kinetics (Figure 5) revealed fast migration of 70% of cesium from the quartz sand surface within 30 min of contact. However, ^{137}Cs leaching was reduced to 0.4–2.5% when composite latex/CoHCF coatings were formed on contaminated surface before it was brought to contact with water (Figure 5A). Figure 5A shows that CoHCF content in the composites used for coating formation can be as low as ~0.01 mmol/g. Despite the latex coatings hydrophility, 10 d of monitoring the ^{137}Cs leaching showed only slight increase of ^{137}Cs content in liquid media indicating long-term stability of the composite coatings (Figure 5B).

At the same content of CoHCF in latex/CoHCF composites (0.014 mmol CoHCF per 1 g of latex, latex solid content 2%), the efficiency of coatings in ^{137}Cs fixation was higher for

BMADS-0.3-based composite that correlates with the coatings thickness (Table 2). Although the volume fraction of the sorbent (CoHCF) is lower in thicker BMADS-0.3/CoHCF composite coating, the longer ionic pathway is, most likely, beneficial to minimize cesium leaching caused by the coating defects.

SEM images of the latex coatings and composite coatings demonstrate a significant difference in their surface topography (Figure 6). Hybrid coatings formed by BMMDS-0.3 and BMADS-0.3 latexes are rougher than original latex coatings and exhibit small hole defects, which can originate from the high interfacial tension between polymer and inorganic nanoparticles. Note that we were not aimed here to optimize film forming properties of the latexes, so no coalescing aids were added to avoid any interference with composite formation that could complicate data interpretation. SEM images also show that distribution of CoHCF nanoparticles in dry composite

coatings is not perfectly homogeneous (Figure 6) but their crystal size remains in nanoscale range. XRD patterns of coatings exhibit only weak reflections of CoHCF typical for nanosized crystals (Supporting Information, Figure S6).

According to the data shown in Table 2 (lines 4, 5, 9, 10), ^{137}Cs leaching can be minimized by increasing thickness BMMDS-0.3 and BMADS-0.3 composite coatings. The films cast from composite dispersions with latex solid contents of 5% and 10% and fixed CoHCF content per 1 g of latex showed significantly lower rate of ^{137}Cs leaching. Thus, both latex types—containing carboxylic and amino groups—can be used for fabrication of composite coatings for cesium fixation.

The important issue for environmental applications of such composite coatings is their performance in the presence of other cations. Transition metal hexacyanoferrates (II) are very selective to cesium ions but sensitive to the presence of sodium and potassium ions at high concentrations.[17] We have previously shown that ^{137}Cs distribution coefficients for latex/CoHCF composites in dispersions remained sufficiently high even in 2 M NaCl solution, while ^{137}Cs distribution coefficients for composite materials obtained by electrochemical deposition of latex/CoHCF on carbon fibers dropped significantly already in 0.1 M NaCl solution.[8] The most probable reason for this effect is the difference in sodium ion concentration inside and outside latex film due to the existence of the Donnan potential. Since this effect is more pronounced for cation-exchangers (carboxylic latexes), migration of ^{137}Cs from BMMDS-0.3/CoHCF composite coatings to liquid media increases from 5.6% in 0.1 M NaCl to ~10% in 0.5 M NaCl within 24 h (Table 2, lines 2−3, 7−8). However, the concentration of sodium ions in the environment (in soil and ground waters), aside from sea-coastal areas, is substantially lower than 0.1 M, and, thus, shall not significantly decrease efficiency of latex/CoHCF composite coatings.

4. CONCLUSIONS

Preventing migration of radionuclides from contaminated solid surfaces into environment after nuclear accidents remains a challenging task. Application of polymeric dust suppressors helps to securely eliminate migration of radionuclides with aerosols but does not limit their mobility under contact with atmospheric precipitates, ground, and soil waters due to solubility and/or permeability of polymeric fixatives. Thus, long-term open-air application of conventional fixatives is associated with radionuclide migration from soil surface downward into the soil profile that significantly increase volume of soil, which must be removed or decontaminated. Here we have presented a new concept to form composite fixative coatings on radioactively contaminated surfaces, which, due to combination of dust-suppressing properties of film-forming latexes and selective sorption properties of nanosized sorbents, can eliminate migration of radionuclides with both aerosols and surface and ground waters.

Here we have demonstrated fabrication of composite coatings for fixation of cesium radionuclides using colloidal stable latex/cobalt hexacyanoferrate(II) (CoHCF). A series of latex/CoHCF containing amino and carboxylic functional groups has been synthesized and used for latex/CoHCF composites fabrication. We have shown that the optimal concentration of −COOH groups on the surface of carboxylic latexes for latex/CoHCF fabrication is close to 1 mmol per 1g of latex, while amino-latexes containing only 0.1 mmol −NH$_2$

groups per 1g of latex can be used due to the electrostatic contribution to composite stabilization in the latter case.

Composite coatings for cesium fixation have been fabricated on ^{137}Cs-contaminated sand by casting colloidal stable latex/CoHCF composites with various CoHCF contents. After exposure of contaminated sand it was found that ^{137}Cs leaching with water from contaminated sand coated with latex/CoHCF composites can be reduced to 0.4%, whereas coatings formed by original latexes allows fast migration of 70% of cesium from the surface within 30 min. [137]Cs migration from the surface was efficiently eliminated when the latex/CoHCF composites containing only ~0.01 mmol CoHCF per 1 g of latex were used. 10 d of monitoring the ^{137}Cs leaching has shown only slight increase of the cesium content in liquid media indicating long-term stability of the composite coatings.

An important advantage of such approach consists in the possibility to use commercially available dust-suppressors, which are mainly carboxylic latexes, and modify their properties by addition of relatively low amount of selective inorganic materials, which does not significantly increase production costs but opens a window for fabrication of coatings for entrapment of a wide range of target radionuclides, if appropriate nanosized selective sorbents are used.

■ ASSOCIATED CONTENT

Ⓢ Supporting Information

Compositions of the reaction mixture used for latex synthesis (Table S1), electrokinetic properties of latexes (ζ-potential vs pH); size distributions and DLS correlation functions for original latexes and latex/CoHCF composites, kinetics of cobalt hexacyanoferrate(II) settling in amino latex/CoHCF composite dispersions and carboxylic latex/CoHCF composites with different CoHCF content;; XRD patterns of latex/CoHCF composites (Figures S1−6S). This material is available free of charge via the Internet at http://pubs.acs.org.

■ AUTHOR INFORMATION

Corresponding Author
*Telephone: +7-423-2311889. E-mail: sbratska@ich.dvo.ru.
Author Contributions
The manuscript was written through contributions of all authors. All authors have given approval to the final version of the manuscript.
Notes
The authors declare no competing financial interest.

■ ACKNOWLEDGMENTS

■ REFERENCES

(1) Zengeni, E.; Hartmann, P. C.; Pasch, H. Encapsulation of Clay by Ad-Miniemulsion Polymerization: The Influence of Clay Size and Modifier Reactivity on Latex Morphology and Physical Properties. *ACS Appl. Mater. Interfaces* **2012**, *4*, 6956−6967.
(2) Wen, N.; Tang, Q.; Chena, M.; Wu, L. Synthesis of PVAc/SiO$_2$ Latices Stabilized by Silica Nanoparticles. *J. Colloid Interface Sci.* **2008**, *320*, 152−158.

(3) Watanabe, M.; Minami, Y.; Masuyama, A.; Matsukawa, K. Hybrid Films Prepared from Latex Particles Incorporating Metal Oxide Nanoparticles. *Res. Chem. Intermed.* **2013**, *39*, 291−300.

(4) Liu, W. J.; He, W. D.; Wang, Y. M.; Wang, D.; Zhang, Z. C. New Approach to Hybrid Materials: Functional Sub-micrometer Core/shell Particles Coated with NiS Clusters by γ-irradiation. *Polymer* **2005**, *46*, 8366−8372.

(5) Wada, T.; Uragami, T. Preparation and Characteristics of a Waterborne Preventive Stain Coating Material with Organic-Inorganic Composites. *JCT Res.* **2006**, *3*, 267−274.

(6) Zhou, X. D.; Chen, F.; Yang, J. T.; Yan, X. H.; Zhong, M. Q. Preparation and Self-Sterilizing Properties of Ag@TiO2−Styrene−Acrylic Complex Coatings. *Mater. Sci. Eng.* **2013**, *C 33*, 1209−1213.

(7) Surbeck, H. Alpha Spectrometry Sample Preparation using Selectively Adsorbing thin Films. *Appl. Radiat. Isot.* **2000**, *53*, 97−100.

(8) Avramenko, V.; Bratskaya, S.; Zheleznov, V.; Sheveleva, I.; Voitenko, O.; Sergienko, V. Colloid Stable Sorbents for Cesium Removal: Preparation and Application of Latex Particles Functionalized with Transition Metals Ferrocyanides. *J. Hazard. Mater.* **2011**, *186*, 1343−1350.

(9) Parra, R. R.; Medina, V. F.; Conca, J. L. The Use of Fixatives for Response to a Radiation Dispersal Devise Attack - a Review of the Current (2009) State-of-the-Art. *J. Environ. Radioact.* **2009**, *100*, 923−934.

(10) Andersson, K. G.; Roed, J. Removal of Radioactive Fallout from Surface of Soil and Grassed Surfaces using Peelable Coatings. *J. Environ. Radioact.* **1994**, *22*, 197−203.

(11) Klyuchnikov, A. A.; Krasnov, V. A.; Rud'ko, V. M.; Shcherbin, V. N. Ob'ekt "Ukrytie" 1986−2006 ("Shelter" 1986−2006): Chernobyl. *IPB AES NAN Ukrainy* **2006**, 168.

(12) Nakano, M.; Yong, R. N. Overview of Rehabilitation Schemes for Farmlands Contaminated with Radioactive Cesium Released from Fukushima Power Plant. *Eng. Geol. (Amsterdam, Neth.)* **2013**, *155*, 87−93.

(13) Fujiwara, T.; Saito, T.; Muroya, Y.; Sawahata, H.; Yamashita, Y.; Nagasaki, S.; Okamoto, K.; Takahashi, H.; Uesaka, M.; Katsumura, Y.; Tanaka, S. Isotopic Ratio and Vertical Distribution of Radionuclides in Soil Affected by the Accident of Fukushima Dai-ichi Nuclear Power Plants. *J. Environ. Radioact.* **2012**, *113*, 37−44.

(14) *Handbook of Parameter Values for the Prediction of Radionuclide Transfer Terrestrial and Freshwater Environments;* Technical Reports Series 472; IAEA: Vienna, Austria, 2010.

(15) Shand, C. A.; Rosén, K.; Thored, K.; Wendler, R.; Hillier, S. Downward Migration of Radiocaesium in Organic Soils Across a Transect in Scotland. *J. Environ. Radioact.* **2013**, *115*, 124−133.

(16) Andersson, K. *The Characterization and Removal of Chernobyl Debris in Garden Soils;* Riso-M-2912: Riso Library, Riso National Laboratory: Roskilde, Denmark, 1991.

(17) Haas, P. A. A Review of Information on Ferrocyanide Solids for Removal of Cesium from Solutions. *Sep. Sci. Technol.* **1993**, *28*, 2479−2506.

(18) Musyanovych, A.; Rossmanith, R.; Tontsch, C.; Landfester, K. Effect of Hydrophilic Comonomer and Surfactant Type on the Colloidal Stability and Size Distribution of Carboxyl- and Amino-Functionalized Polystyrene Particles Prepared by Miniemulsion Polymerization. *Langmuir* **2007**, *23*, 5367−5376.

(19) Jansat, S.; Pelzer, K.; Garcia-Anton, J.; Raucoules, R.; Philippot, K.; Maisonnat, A.; Chaudret, B.; Guari, Y.; Mehdi, A.; Reye, C.; Corriu, R.J. R. Synthesis of New RuO$_2$@SiO$_2$ Composite Nanomaterials and their Application as Catalytic Filters for Selective Gas Detection. *Adv. Funct. Mater.* **2007**, *17*, 3339−3347.

(20) Khutoryanskiy, V. V.; Nurkeeva, Z. S.; Mun, G. A.; Sergaziyev, A. D.; Kadlubowski, S.; Fefelova, N. A.; Baizhumanova, T.; Rosiak, J. M. Temperature-Responsive Linear Polyelectrolytes and Hydrogels Based on [2-(methacryloyloxy)ethyl] trimethylammonium chloride and N-isopropylacrylamide and Their Complex Formation with Potassium Hexacyanoferrates (II, III). *J. Polym. Sci., Part B: Polym. Phys.* **2004**, *42*, 515−522.

(21) Watanabe, M.; Toshiyuki, T. Acrylic Polymer/Silica Organic-Inorganic Hybrid Emulsions for Coating Materials: Role of the Silane Coupling Agent. *J. Polym. Sci., Part A: Polym. Chem.* **2006**, *44*, 4736−4742.

(22) Zou, M. X.; Wang, S. J.; Zhang, Z. C.; Ge, X. W. Preparation and Characterization of Polysiloxane-poly(butyl acrylate-styrene) Composite Latices and Their Film Properties. *Eur. Polym. J.* **2005**, *41*, 2602−2613.